Chapter 5
Diamond D_5

Csaba L. Nagy and Mircea V. Diudea

Abstract Carbon allotropes, built up as hyper-structures of the classical diamond and having a high percentage of sp^3 carbon atoms and pentagons, are generically called diamond D_5. Four allotropes are discussed in this chapter: a spongy net; a dense hyper-diamond D_5, with an "anti"-diamantane structure; the corresponding hyper-lonsdaleite; and a quasi-diamond which is a fivefold symmetry quasicrystal with "sin"-diamantane structure. Substructures of these allotropes are presented as possible intermediates in a lab synthesis, and their energetics evaluated at Hartree-Fock, DFT, and DFTB levels of theory. A topological description of these networks is also given.

5.1 Introduction

Nano-era, a period starting since 1985 with the discovery of C_{60}, is dominated by the carbon allotropes, studied for applications in nanotechnology. Among the carbon structures, fullerenes (zero dimensional), nanotubes (one dimensional), graphenes (two dimensional), diamonds, and spongy nanostructures (three dimensional) were the most studied (Diudea and Nagy 2007). Inorganic compounds also attracted the attention of scientists. Recent articles in crystallography promoted the idea of topological description and classification of crystal structures (Blatov et al. 2004, 2007, 2009; Delgado-Friedrichs and O'Keeffe 2005).

Dendrimers are hyper-branched nanostructures, made by a large number of (one or more types) substructures called monomers, synthetically joined within a rigorously tailored architecture (Diudea and Katona 1999; Newkome et al. 1985;

C.L. Nagy (✉) • M.V. Diudea (✉)
Department of Chemistry, Faculty of Chemistry and Chemical Engineering, Babes-Bolyai University, Arany Janos street 11, Cluj RO-400028, Romania
e-mail: nc35@chem.ubbcluj.ro; diudea@chem.ubbcluj.ro

M.V. Diudea and C.L. Nagy (eds.), *Diamond and Related Nanostructures*, Carbon Materials: Chemistry and Physics 6, DOI 10.1007/978-94-007-6371-5_5,

Tomalia 1993). They can be functionalized at terminal branches, thus finding a broad pallet of applications in chemistry, medicine, etc. (Tang et al. 1996; Pan et al. 2007).

Multi-tori are structures of high genera (Diudea 2005b, 2010b; Diudea and Nagy 2007), consisting of more than one tubular ring. Such structures can appear in spongy carbon or in zeolites (DeCarli and Jamieson 1961; Aleksenski et al. 1997; Krüger et al. 2005). Spongy carbon has recently been synthesized (Benedek et al. 2003; Barborini et al. 2002).

There are rigid monomers that can self-assemble in dendrimers, but the growing process stops rather at the first generation. At a second generation, yet the endings of repeat units are not free, they fit to each other, thus forming either an infinite lattice, if the monomer symmetry is octahedral, or a spherical multi-torus, if the symmetry is tetrahedral. The last one is the case of structures previously discussed by Diudea and Ilic (2011).

A detailed study on a multi-torus (Diudea 2010a; Diudea and Ilic 2011), built up by a tetrapodal monomer designed by $Trs(P_4(T))$ sequence of map operations (Diudea 2005a, b; Diudea et al. 2006) and consisting of all pentagonal faces, revealed its dendrimer-like structure (given as the number of monomer units added at each generation, in a dendrimer divergent synthesis, up to the 5th one): 1; 4; 12, 24, 12, 4. Starting with the second generation (i.e., the stage when first 12 monomers were added), pentagonal super-rings appear, leading finally to the multi-torus. The above sequence will be used to suggest a synthetic way to the multi-cage C_{57}, which is the reduced graph of the above multi-torus and one of the main substructures of the diamond D_5.

This chapter is organized as follows: after a short introduction, the main substructures of the D_5 diamonds are presented in Sect. 5.2, while the networks structure is detailed in Sect. 5.3. The next section provides a topological description of the nets, and computational details are given in Sect. 5.5. The chapter ends with conclusions and references.

5.2 Main Substructures of D_5

Carbon allotropes, built up as hyper-structures of the classical diamond and having a high percentage of sp^3 carbon atoms and pentagons, are generically called *diamond D_5* (Diudea 2010a, b; Diudea and Nagy 2012; Diudea et al. 2012). The most important substructures, possible intermediates in the synthesis of D_5, are detailed in the following.

5.2.1 Structure C_{57}

Structure C_{57}, above mentioned, can be "composed" by condensing four C_{20} cages so that they share a common vertex. Starting from a tetrahedral configuration,

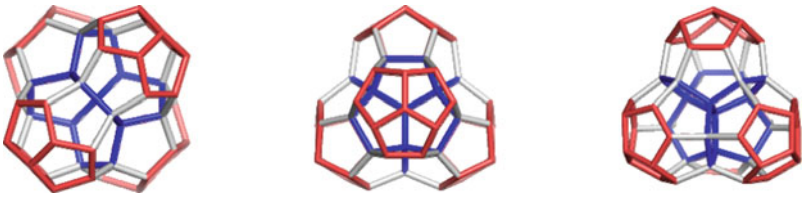

C_2 axe view C_3 axe view side view

Fig. 5.1 C_{57} multi-cage in different views

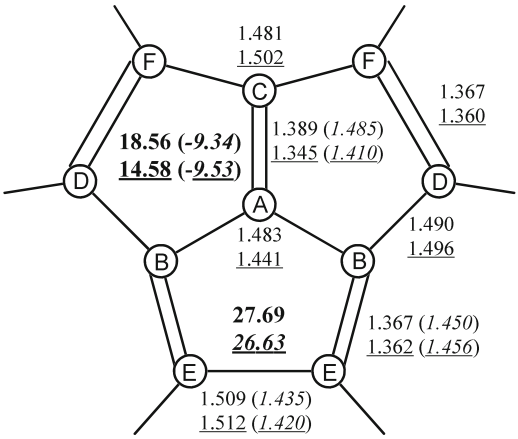

Fig. 5.2 Bond lengths and NICS values (*boldface*) in the acepentalene fragment for C_{57}-D_{2d} and C_{57}^{8-}-T_d (*italics*) and in $C_{10}H_6$-C_s (*underlined*) and $C_{10}H_6^{2-}$-C_{3v} (*italics*) obtained at the B3LYP/6-311G(2d,p) level of theory

geometry optimization of C_{57}, without symmetry constraints, leads to a structure with D_{2d} symmetry. The deformation occurs because of the degeneracy of the frontier orbitals. Maximal symmetry can be achieved by an *octa*-anionic form. This can be explained if we consider C_{57} consisting of two fragments: the core (in blue, Fig. 5.1), i.e., the centrohexaquinane C_{17} (Fig. 5.4 – Paquette and Vazeux 1981; Kuck 2006) which is capped by four acepentalene (Haag et al. 1996) fragments (consisting of only three-valence carbon atoms – marked in red, Fig. 5.1). A theoretical study (Zywietz et al. 1998) has shown the ground state of acepentalene $C_{10}H_6$ with 10π electrons has C_s symmetry. Since in C_{57} the four acepentalene fragments are isolated from each other, their local geometry is close to the isolated acepentalene molecule. The dianion of acepentalene, with 12π electrons, is a stable and aromatic structure ($C_{10}H_6^{2-}$-C_{3v}) and has been isolated as salts (Haag et al. 1998). If two electrons are added for each acepentalene fragment, the geometry optimization resulted in a structure with tetrahedral symmetry C_{57}^{8-}-T_d.

Figure 5.2 summarizes the geometry and local ring aromaticity in the acepentalene fragments of C_{57} and its anion (in italics) compared to that of acepentalene (underlined values) and its dianion (in italics). It can be seen that in C_{57} the bonds are in general slightly longer than in its octa-anionic form, where the bond

Table 5.1 Local strain energies (kcal mol^{-1}) according to POAV theory, computed for the three-coordinated carbon atoms in the acepentalene fragment

	C_{57}-D_{2d}	$C_{10}H_6$-C_s	C_{57}^{8-}-T_d	$C_{10}H_6^{2-}$-C_{3v}
A	37.359	17.974	42.695	8.233
B	25.778	8.506	18.792	6.118
C	17.198	3.161	18.792	6.118
D	19.458	0.003	22.654	0.072
E	19.703	1.246	22.654	0.072
F	22.032	0.002	22.654	0.072

Labeling of the atoms position corresponds to that in Fig. 5.1

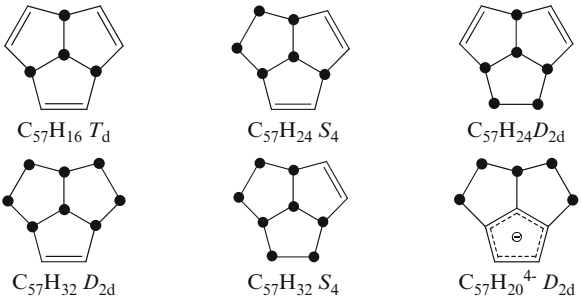

Fig. 5.3 Patterns of the partially hydrogenated C_{57} structure. The *black dots* correspond to the linking position of the hydrogen atoms in the acepentalene fragment

lengths are nearly uniform, ranging from 1.43 to 1.48 Å. Notice the central bonds (AB = AC = 1.48) are much longer in C_{57} than in $C_{10}H_6^{2-}$, with implications in the pyramidalization of the central atom "A" (see below).

The NICS study revealed that, in C_{57}^{8-}, the fragment is aromatic and nearly the same as the acepentalene dianion. However these rings are more antiaromatic in C_{57} than in $C_{10}H_6$-C_s.

The local strain energy of the three-coordinated atoms, induced by deviation from planarity, was evaluated by the POAV theory (Haddon 1987, 1990) and is presented in Table 5.1. Notice that both in C_{57} and its anionic form there is a big strain on each atom compared to the isolated acepentalene. The central atom "A" has the largest strain and becomes a reactive site, particularly in case of C_{57}^{8-}; this polar atom is then pushed away from the molecule, and therefore the C_{20} moieties have an elongated shape.

Strain relief could be achieved by partial or total hydrogenation (in general, exohedral derivatization). There are known examples of non-IPR fullerenes that are stabilized by hydrogenation/halogenation of their pentagon double/triple substructures (Wahl et al. 2006; Prinzbach et al. 2006; Chen et al. 2004; Fowler and Heine 2001; Han et al. 2008). Patterns appearing in the partially hydrogenated C_{57} structure are illustrated in Fig. 5.3.

All possible isomers in the addition of hydrogen to C_{57} were checked: an even number of hydrogen atoms (with one exception) were added to each acepentalene fragment, from four up to ten (i.e., complete reduced species), only the lowest energy isomers being illustrated in Fig. 5.3. Exception was the case when added

Table 5.2 Single-point calculation results (HOMO-LUMO gap in eV and total energy E_{tot} in a.u.) for the C_{57} multi-cage and the hydrogenated $C_{57}H_n$ derivatives, calculated at the HF/6-31G(d,p) and B3LYP/6-31G(d,p) levels of theory

		HF			B3LYP		
Structure	PG	Gap	E_{tot} (au)	E_{tot}/C	Gap (eV)	E_{tot} (au)	E_{tot}/C
C_{57}	D_{2d}	7.57	−2,156.98	−37.84	1.89	−2,196.27	−38.53
C_{57}^{8-}	T_d	7.91	−2,154.27	−37.79	3.12	−2,168.24	−38.04
$C_{57}H_{16}$	T_d	11.55	−2,167.19	−38.02	4.84	−2,181.06	−38.26
$C_{57}H_{20}^{4-}$	D_{2d}	10.43	−2,169.01	−38.05	4.37	−2,183.13	−38.30
$C_{57}H_{24}$	D_{2d}	11.31	−2,172.15	−38.11	4.78	−2,186.15	−38.35
$C_{57}H_{24}$	S_4	11.44	−2,172.15	−38.11	4.83	−2,186.15	−38.35
$C_{57}H_{32}$	D_{2d}	12.10	−2,177.08	−38.19	5.27	−2,191.22	−38.44
$C_{57}H_{32}$	S_4	12.11	−2,177.08	−38.19	5.32	−2,191.22	−38.44
$C_{57}H_{40}$	T_d	14.27	−2,181.99	−38.28	7.37	−2,170.67	−38.08

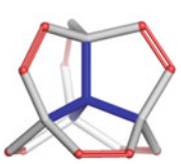

$C_{17}H_{12}$-T_d (1,4,12)

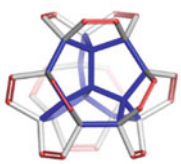

$C_{41}H_{24}$-T_d (1,4,12,24)

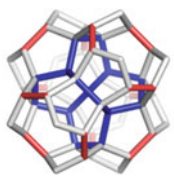

$C_{53}H_{24}$-C_{2v} (1,4,12,24,12)

Fig. 5.4 Structures in the pathway to C_{57} (1; 4; 12, 24, 12, 4); the number of atoms added shell by shell is given in *brackets*

five hydrogen atoms and one electron, thus resulting an isomer with one aromatic pentagon in each acepentalene fragment. Both $C_{57}H_{24}$ and $C_{57}H_{32}$ have two isomers, with symmetries D_{2d} and S_4, respectively, and very close stability (the difference in their total energy is only 0.01 kcal/mol, while in the HOMO-LUMO gap is 0.05 eV). In the totally reduced species $C_{57}H_{40}$, the bond lengths are in the range of 1.52 (core)–1.56 Å (periphery) compared to 1.55 Å in the dodecahedrane, so that the C_{20} fragments regain a quasi-spherical shape. Single-point calculations for hydrogenated $C_{57}H_n$ derivatives are listed in Table 5.2.

The stabilization by hydrogenation is more pregnant in case of C_{20}; while dodecahedrane $C_{20}H_{20}$ was synthesized in amounts of grams, the efforts of scientists to prove the existence of the smallest fullerene C_{20} are well-known (Paquette and Balogh 1982; Prinzbach et al. 2006).

Possible intermediates in the pathway to C_{57} molecule, starting from C_{17} considered the "seed" of D_5, are presented in Fig. 5.4, while the single-point calculation data are shown in Table 5.3. These species could be used as derivatives (e.g., halogenated and hydrogenated ones) in the building of further structures. Their stability was evaluated as partially hydrogenated species, the red bonds in Fig. 5.4 being kept as double bonds. The vibrational spectra of these molecules evidenced a very rigid carbon skeleton, only the hydrogen atoms presenting intense signals.

Table 5.3 Single-point calculation results (HOMO-LUMO gap in eV and total energy E_{tot} in a.u.) for intermediate structures leading to C_{57} multi-cage, calculated at the HF/6-31G(d,p) and B3LYP/6-31G(d,p) levels of theory

		HF			B3LYP		
Structure	PG	Gap	E_{tot} (au)	E_{tot}/C	Gap	E_{tot} (au)	E_{tot}/C
$C_{17}H_{12}$	T_d	12.99	−650.66	−38.27	6.04	−654.92	−38.52
$C_{41}H_{24}$	T_d	12.59	−1,566.40	−38.20	5.75	−1,576.58	−38.45
$C_{53}H_{24}$	T_d	11.62	−2,020.50	−38.12	4.97	−2,033.59	−38.37
$C_{65}H_{24}$	T_d	10.15	−2,474.64	−38.07	3.78	−2,490.58	−38.32
$C_{81}H_{40}$	T_d	12.99	−3,090.56	−38.16	6.03	−3,110.51	−38.40

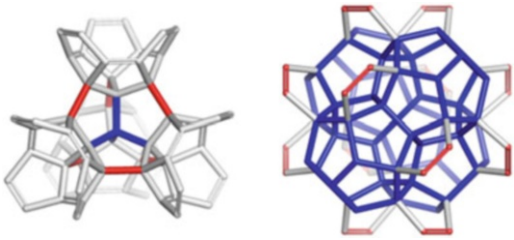

$C_{65}H_{24}$-T_d $C_{81}H_{40}$-T_d

Fig. 5.5 Intermediate structures to D_5 network

Of particular interest are the outer (red) bonds in C_{17}, the length of which varying by the structure complexity. As the structure grows, an increase in their strain appears provoking an elongation of the mentioned bond. This can be observed in the increase of the total energy per carbon atom (and decrease of the gap energy) in the order $C_{17} > C_{41} > C_{53}$. However, with further addition of C_1/C_2 fragments, finally leading to a periodic network (see below), the considered bonds are shortened progressively.

A way from C_{57} to D_5 could include C_{65} and C_{81} intermediates (see Fig. 5.5). The stability of these structures was evaluated as hydrogenated species (Table 5.3, the last two rows). The structure C_{81} (with a C_{57} core and additional 12 flaps) is the monomer of spongy D_5 network (see below). Its stability is comparable to that of the reduced C_{17} seed (Table 5.3, first row) and also to that of the fully reduced C_{57} (Table 5.2, last row), thus supporting the viability of the spongy lattice.

5.2.2 Hyper-Adamantane

Other substructures/intermediates, related to D_5, could appear starting from C_{17}. The seed C_{17} can dimerize (probably by a cycloaddition reaction) to $C_{34}H_{12}$ (Fig. 5.6), a C_{20} derivative bearing 2×3 pentagonal wings in opposite polar disposition. The dimer can further form an angular structure C_{51} (Fig. 5.6, right).

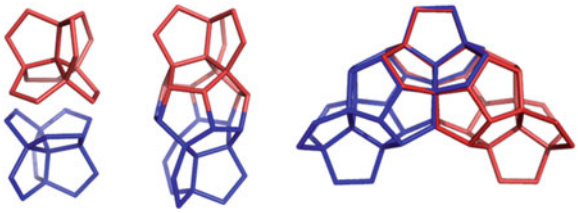

Fig. 5.6 Steps to ada_20: C_{17} (*left*) dimerizes to $C_{34}H_{12}$ (*middle*) and trimerizes to $C_{51}H_{14}$ (*right*)

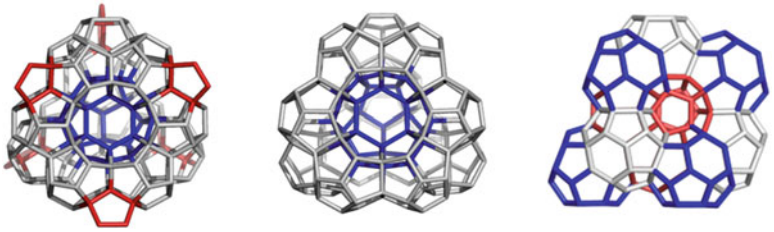

Fig. 5.7 Adamantane-like structures: ada_20_170 (*left*), ada_20_158 (*central*), and ada_28_213 (*right*)

Table 5.4 Single-point calculation results (HOMO-LUMO gap in eV and total energy E_{tot} in a.u.) at the B3LYP/6-31G(d,p) level of theory for some substructures of D_5

Formula	Symmetry	GAP (eV)	E_{tot}/N (a.u.)
$C_{17}H_{12}$	T_d	6.04	−38.52
$C_{34}H_{12}$	D_{3d}	3.236	−38.305
$C_{51}H_{14}$	C_{2v}	3.340	−38.257
$C_{57}H_{18}$	D_{3h}	2.969	−38.282
$C_{170}H_{12}$	T_d	3.171	−38.136
$C_{158}H_{12}(D_5\_20)$	T_d	3.236	−38.139
$C_{213}H_{28}(D_5\_28)$	T_d	3.696	−38.180
$C_{250}H_{30}$ (L_5_28)	D_{3h}	0.333	−38.172
$C_{134}H_{20}$	D_{3d}	3.738	−38.188

A linear analogue is energetically also possible. The angular tetramer C_{51} will compose the six edges of a tetrahedron in forming an adamantane-like **ada_20_170**, with six pentagonal wings (in red – Fig. 5.7, left) or without wings, as in **ada_20_158** (Fig. 5.7, central). Energetic data for these intermediates are given in Table 5.4. The unit ada_20_158 consist of $12 \times C_{20}$ cages, the central hollow of which exactly fitting the structure of fullerene C_{28}. A complete tetrahedral ada_20_196 consist of $16 \times C_{20}$ or $4 \times C_{57}$ units. The hyper-adamantane is the repeating unit of the dense diamond D_5 (see below). A corresponding ada_28_213 can be conceived starting from C_{28} (Fig. 5.7, right).

In the above symbols, "20" refers to C_{20}, as the basic cage in the frame of dense diamond D_5 (see below), while the last number counts the carbon atoms in the structures.

5.3 Diamond D_5 Allotropes

Four different allotropes can be designed, as will be presented in the following.

5.3.1 Spongy Diamond D_5

In spongy diamond D_5 (Fig. 5.8), the nodes of the network consist of alternating oriented (colored in red/blue) C_{57} units; the junction between two nodes recalls a C_{20} cage. The translational cell is a cube of eight C_{57} entities. This network is a decoration of the P-type surface; it is a new 7-nodal 3,3,4,4,4,4,4-c net, group *Fm*-3*m*; point symbol for net: $(5^3)16(5^5.8)36(5^6)17$; stoichiometry (3-c)4(3-c)12(4-c)24(4-c)12(4-c)12(4-c)4(4-c).

The density of the net varies around an average of $d = 1.6$ g/cm^3, in agreement with the "spongy" structure illustrated in Fig. 5.8.

5.3.2 Diamond D_5

The ada_20 units can self-arrange in the net of dense diamond D_5 (Fig. 5.9, left). As any net has its co-net, the diamond D_5_20 net has the co-net D_5_28 (Fig. 5.9, right), with its corresponding **ada_28_213** unit (Fig. 5.7, right). In fact it is one and the same *triple periodic* D_5 network, built up basically from C_{20} and having as hollows the fullerene C_{28}.

This dominant pentagon-ring diamond (Fig. 5.8) is the *mtn* triple periodic, three-nodal net, namely, ZSM-39, or clathrate II, of point symbol net: {5^5.6}12{5^6}5 and $2[5^{12}]$; $[5^{12}.6^4]$ tiling, and it belongs to the space group: *Fd*-3*m*. For all the crystallographic data, the authors acknowledge Professor Davide Proserpio, University of Milan, Italy.

Domains of this diamond network, namely, D_5_20_3,3,3_860 and D_5_28_3,3,3_1022 co-net, were optimized at the DFTB level of theory (Elstner et al. 1998).

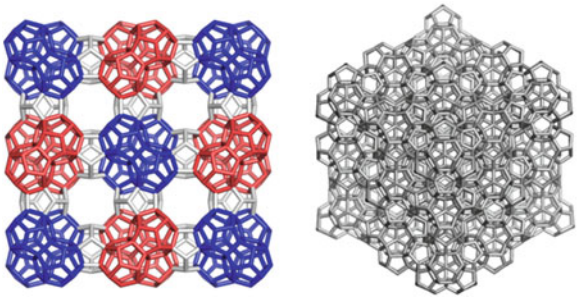

top view corner view

Fig. 5.8 Spongy D_5 (C_{57}) triple periodic network

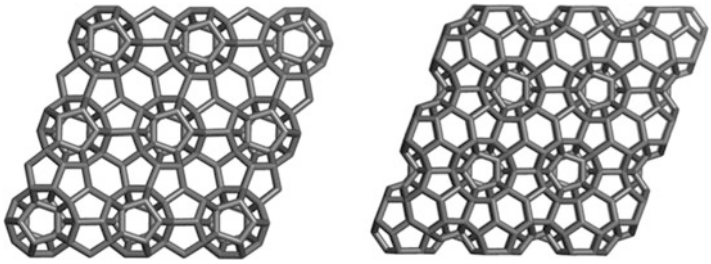

Fig. 5.9 Diamond D_5_20 net and its co-net D_5_28 represented as (*k*,*k*,*k*)-cubic domains: D_5_20_3,3,3_860 (*left*) and D_5_28_3,3,3_1022 (*right*); "*k*" is the number of repeating units on each edge of the domain

Hydrogen atoms were added to the external carbon atoms of the network structures, in order to keep the charge neutrality and the sp^3 character of the C–C bonds at the network surface. Energetically stable geometry structures were obtained in both cases, provided the same repeating unit was considered.

Identification of the equivalent carbon atoms in the neighboring units of the $3 \times 3 \times 3$ super-cell along the main symmetry axes, envisaged a well-defined triclinic lattice, with the following parameters: $a = b = c = 6.79$ Å and $\alpha = 60°$, $\beta = 120°$, $\gamma = 120°$, even the most symmetrical structure is *fcc* one. Density of the D_5 network was calculated to be around 2.8 g/cm^3.

Analyzing the C–C bond distances in these carbon networks, the values vary in a very narrow distance domain of 1.50–1.58 Å, suggesting all carbon atoms are sp^3 hybridized. Considering the one-electron energy levels of the HOMO and LUMO, a large energy gap could be observed for both D_5_20_860 net ($E_{HOMO} = -5.96$ eV, $E_{LUMO} = +2.10$ eV, $\Delta E_{HOMO-LUMO} = 8.06$ eV) and D_5_28_1022 co-net ($E_{HOMO} = -6.06$ eV, $E_{LUMO} = +2.45$ eV, $\Delta E_{HOMO-LUMO} = 8.51$ eV) structures, which indicates an insulating behavior for this carbon network.

Structural stability of substructures related to the D_5 diamond was evaluated both in static and dynamic temperature conditions by molecular dynamics MD (Kyani and Diudea 2012; Szefler and Diudea 2012). Results show that C_{17} is the most temperature resistant fragment. For a detailed discussion, see Chap. 7.

Note that the hypothetical diamond D_5 is also known as *fcc*-C_{34} because of its face-centered cubic lattice (Benedek and Colombo 1996). Also note that the corresponding clathrate structures are known in silica synthetic zeolite ZSM-39 (Adams et al. 1994; Meier and Olson 1992; Böhme et al. 2007) and in germanium allotrope Ge(*cF*136) (Guloy et al. 2006; Schwarz et al. 2008) as real substances.

5.3.3 *Lonsdaleite L_5*

Alternatively, a hyper-lonsdaleite L_5_28 network (Fig. 5.10, left) can be built (Diudea et al. 2011, 2012) from hyper-hexagons L_5_28_134 (Fig. 5.10, right), of

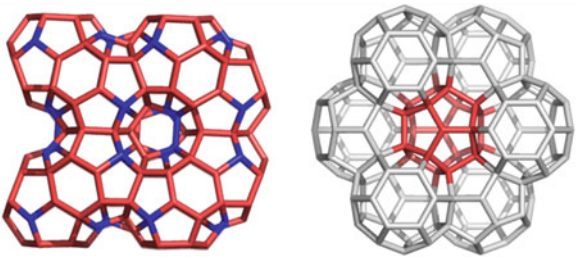

Fig. 5.10 Lonsdaleite L_5_28 net represented as L_5_28_250 (side view – *left*); the substructure L_5_28_134 is a hyper-hexagon of which nodes are C_{28} with additional two C atoms, thus forming a C_{20} core (*top view – central*); the L_5_20 co-net (in *red*) superimposes partially over the net of D_5_20 (*side view – right*) in the domain (*k*,*k*,2)

which nodes represent C_{28} fullerenes, joined by identifying the four tetrahedrally oriented hexagons of neighboring cages. The lonsdaleite L_5_28/20 is a triple periodic network, partially superimposed to the D_5_20/28 net. Energetic data for the structures in Fig. 5.10 are given in Table 5.4.

5.3.4 Quasi-Diamond D_5

A fourth allotrope of D_5 was revealed by Diudea (Chap. 19) as D_5_*sin* quasicrystal diamond (Fig. 5.11), clearly different from the "classical" D_5, named here D_5_*anti*. The quasi-diamond D_5_*sin* is a quasicrystal 27 nodal 3,4-c net, of the *Pm* group, with the point symbol: $\{5^3\}18\{5^5.6\}18\ \{5^5.8\}16\{5^6\}13$. Substructures of this new allotrope are shown in the top of Fig. 5.11.

5.4 Topological Description

Topology of diamond D_5, namely, spongy D_5 (Fig. 5.8) and D_5_*anti* (Fig. 5.9), is presented in Tables 5.5 and 5.6, respectively: formulas to calculate the number of atoms, number of rings *R*, and the limits (at infinity) for the ratio of sp^3 C atoms over the total number of atoms and also the ratio *R*[5] over the total number of rings are given function of *k* that is the number of repeating units in a cuboid (*k*,*k*,*k*). One can see that, in an infinitely large net, the content of sp^3 carbon approaches 0.77 in case of spongy net while it is unity in case of dense diamond D_5.

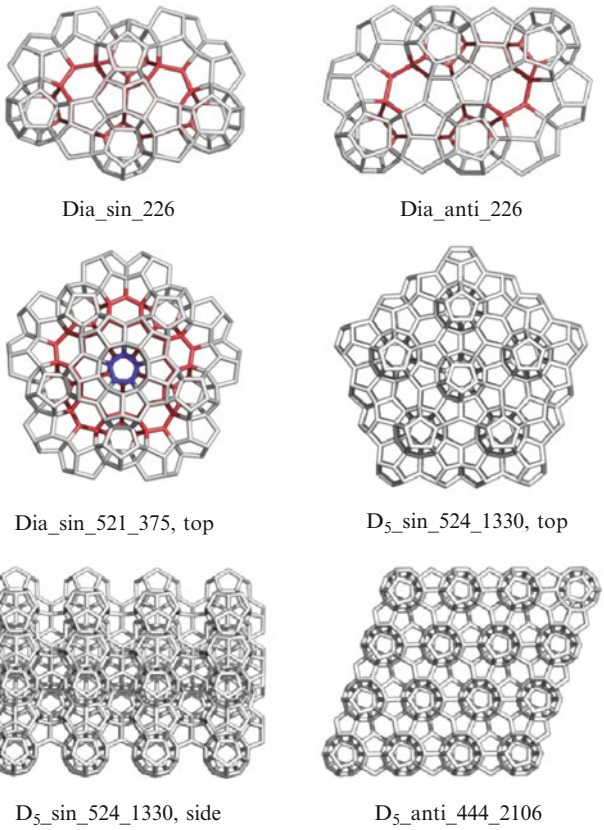

Fig. 5.11 Diamond D_5-related structures

Table 5.5 Topological description (sp^2/sp^3 carbon percentage) of the spongy SD_5 diamond network as function of the number of monomers k

	Formulas: C_{57} net
1	$v(D_5) = 3k^2[19 + 23(k-1)] = 69k^3 - 12k^2$ $e(D_5) = 2k^2(65k - 18); m(D_5) = k^3; k = 1,2,\ldots$
2	$C(sp^2) = 16k^3 - 24k + 48$
3	$C(sp^3) = 53k^3 - 12k^2 + 24k - 48$
4	$C(sp^2\&sp^3) = 69k^3 - 12k^2$
5	$C(sp^3\%) = (53k^3 - 12k^2 + 24k - 48)/(69k^3 - 12k^2)$ $\lim_{k\to\infty}(C(sp^3\%)) = 53/69 \simeq 0.768116$ $\text{Rings}[5] = 6k^2(11k - 4)$
6	$\lim_{k\to\infty}(C(sp^2)/C(sp^3)) = 16/53 \simeq 0.301887$

Table 5.6 Topological description of diamond D_5_20 net function of $k = 1, 2, \ldots$ number of ada_20 units along the edge of a (k,k,k) cuboid

	D_5_20; R[6]; formulas
1	$v(D_5 20a) = -22 - 12k + 34k^3$
2	$\text{Atoms}(sp^3) = -10 - 36k^2 + 34k^3$
3	$R[5] = -18 - 6k - 18k^2 + 36k^3$
4	$R[6] = -1 + 6k - 9k^2 + 4k^3$
5	$R[5] + R[6] = -19 - 27k^2 + 40k^3$
6	$\lim_{k\to\infty} \frac{R[5]}{R[6]} = 9;\ \lim_{k\to\infty} \frac{R[5]}{R[5]+R[6]} = \frac{9}{10}$
7	$\lim_{k\to\infty} \left[\frac{\text{Atoms}(sp^3)}{v(G)} = \frac{-10 - 36k^2 + 34k^3}{-22 - 12k + 34k^3} = \frac{-(10/k^3) - (36/k) + 34}{-(22/k^3) - (12/k^2) + 34} \right] = 1$

5.5 Computational Methods

Geometry optimizations were performed at the Hartree-Fock (HF) and density functional (DFT) levels of theory using the standard polarized double-zeta 6-31G(d,p) basis set. For DFT calculations, the hybrid B3LYP functional was used. Harmonic vibrational frequencies were calculated for all optimized structures at the same level of theory to ensure that true stationary points have been reached. Symmetry was used to simplify calculations after checking the optimizations without symmetry constraints resulted in identical structures. The following discussion only considers the singlet states.

To investigate the local aromaticity, NICS (nucleus-independent chemical shift) was calculated on the DFT optimized geometries. NICS was measured in points of interest using the GIAO (Gauge-Independent Atomic Orbital) method at GIAO-B3LYP/6-311G(2d,p)//B3LYP/6-311G(2d,p). Calculations were performed using the Gaussian 09 package (Gaussian 09 2009).

For larger structures, geometry optimization was performed at SCC-DFTB level of theory (Elstner et al. 1998) by using the DFTB+ program (Aradi et al. 2007) with the numerical conjugated gradient method.

Strain energy, induced by deviation from planarity, appearing in such nanostructures, was evaluated by the POAV theory (Haddon 1987, 1990), implemented in our JSChem software (Nagy and Diudea 2005).

Topological data were calculated by our NanoStudio software (Nagy and Diudea 2009).

5.6 Conclusions

Four allotropes of the diamond D_5 were discussed in this chapter: a spongy net; a dense hyper-diamond D_5, with an "anti"-diamantane structure; the corresponding hyper-lonsdaleite; and a quasi-diamond which is a fivefold symmetry quasicrystal

with "sin"-diamantane structure. The main substructures of these allotropes were presented as possible intermediates in a lab synthesis on the ground of their energetics, evaluated at Hartree-Fock, DFT, and DFTB levels of theory. A topological description of these networks, made in terms of the net parameter *k*, supports the generic name diamond D_5 given to these carbon allotropes; among these, the spongy and quasi-diamond represent novel networks of D_5.

Acknowledgments CL Nagy acknowledges the financial support of the Sectorial Operational Programme for Human Resources Development 2007–2013, cofinanced by the European Social Fund, under the project number POSDRU 89/1.5/S/60189 with the title "Postdoctoral Programs for Sustainable Development in a Knowledge Based Society."

References

Adams GB, O'Keeffe M, Demkov AA, Sankey OF, Huang Y-M (1994) Wide-band-gap Si in open fourfold-coordinated clathrate structures. Phys Rev B 49(12):8048–8053

Aleksenski AE, Baidakova MV, Vul' AY, Davydov VY, Pevtsova YA (1997) Diamond-graphite phase transition in ultradisperse-diamond clusters. Phys Solid State 39:1007–1015

Aradi B, Hourahine B, Frauenheim T (2007) DFTB+, a sparse matrix-based implementation of the DFTB method. J Phys Chem A 111:5678–5684

Barborini E, Piseri P, Milani P, Benedek G, Ducati C, Robertson J (2002) Negatively curved spongy carbon. Appl Phys Lett 81:3359–3361

Benedek G, Colombo L (1996) Hollow diamonds from fullerenes. Mater Sci Forum 232:247–274

Benedek G, Vahedi-Tafreshi H, Barborini E, Piseri P, Milani P, Ducati C, Robertson J (2003) The structure of negatively curved spongy carbon. Diam Relat Mater 12:768–773

Blatov VA, Carlucci L, Ciani G, Proserpio DM (2004) Interpenetrating metal-organic and inorganic 3D networks: a computer-aided systematic investigation. Part I. Analysis of the Cambridge structural database. CrystEngComm 6:377–395

Blatov VA, Delgado-Friedrichs O, O'Keeffe M, Proserpio DM (2007) Three-periodic nets and tilings: natural tilings for nets. Acta Crystallogr Sect A Found Crystallogr 63(5):418–425

Blatov VA, O'Keeffe M, Proserpio DM (2009) Vertex-, face-, point-, Schläfli-, and Delaney-symbols in nets, polyhedra and tilings: recommended terminology. CrystEngComm 12(1): 44–48

Böhme B, Guloy A, Tang Z, Schnelle W, Burkhardt U, Baitinger M, Grin Y (2007) Oxidation of M_4Si_4 (M = Na, K) to clathrates by HCl or H2O. J Am Chem Soc 129:5348–5349

Chen Z, Heine T, Jiao H, Hirsch A, Thiel W, Schleyer PVR (2004) Theoretical studies on the smallest fullerene: from monomer to oligomers and solid states. Chem Eur J 10(4):963–970

DeCarli PS, Jamieson JC (1961) Formation of diamond by explosive shock. Science 133:1821–1822

Delgado-Friedrichs O, O'Keeffe M (2005) Crystal nets as graphs: terminology and definitions. J Solid State Chem 178(8):2480–2485

Diudea MV (ed) (2005a) Nanostructures, novel architecture. NOVA Scientific Publishers, New York

Diudea MV (2005b) Nanoporous carbon allotropes by septupling map operations. J Chem Inf Model 45:1002–1009

Diudea MV (2010a) Diamond D_5, a novel allotrope of carbon. Studia Univ Babes Bolyai Chemia 55(4):11–17

Diudea MV (2010b) Nanomolecules and nanostructures-polynomials and indices, MCM, No. 10. University of Kragujevac, Serbia

Diudea MV, Ilić A (2011) All-pentagonal face multi tori. J Comput Theor Nanosci 8:736–739
Diudea MV, Katona G (1999) Molecular topology of dendrimers. In: Newkome GA (ed) Adv Dendritic Macromol 4(1999):135–201
Diudea MV, Nagy CL (2007) Periodic nanostructures. Springer, Dordrecht
Diudea MV, Nagy CL (2012) C_{20}-related structures: diamond D_5. Diam Relat Mater 23:105–108
Diudea MV, Ştefu M, John PE, Graovac A (2006) Generalized operations on maps. Croat Chem Acta 79:355–362
Diudea MV, Nagy CL, Ilic A (2011) Diamond D_5, a novel class of carbon allotropes. In: Putz MV (ed) Carbon bonding and structures. Carbon materials: chemistry and physics, vol 5. Springer, Dordrecht, pp 273–289
Diudea MV, Nagy CL, Bende A (2012) On diamond D_5. Struct Chem 23:981–986
Elstner M, Porezag D, Jungnickel G, Elsner J, Haugk M, Frauenheim T, Suhai S, Seifert G (1998) Self-consistent-charge density-functional tight-binding method for simulations of complex materials properties. Phys Rev B 58:7260–7268
Fowler PW, Heine T (2001) Stabilisation of pentagon adjacencies in the lower fullerenes by functionalization. J Chem Soc Perkin Trans 2:487–490
Gaussian 09 Rev. A.1, Frisch MJ, Trucks GW, Schlegel HB, Scuseria GE, Robb MA, Cheeseman JR, Scalmani G, Barone V, Mennucci B, Petersson GA, Nakatsuji H, Caricato M, Li X, Hratchian HP, Izmaylov AF, Bloino J, Zheng G, Sonnenberg JL, Hada M, Ehara M, Toyota K, Fukuda R, Hasegawa J, Ishida M, Nakajima T, Honda Y, Kitao O, Nakai H, Vreven T, Montgomery JA, Peralta JE, Ogliaro F, Bearpark M, Heyd JJ, Brothers E, Kudin KN, Staroverov VN, Kobayashi R, Normand J, Raghavachari K, Rendell A, Burant JC, Iyengar SS, Tomasi J, Cossi M, Rega N, Millam NJ, Klene M, Knox JE, Cross JB, Bakken V, Adamo C, Jaramillo J, Gomperts R, Stratmann RE, Yazyev O, Austin AJ, Cammi R, Pomelli C, Ochterski JW, Martin RL, Morokuma K, Zakrzewski VG, Voth GA, Salvador P, Dannenberg JJ, Dapprich S, Daniels AD, Farkas Ö, Foresman JB, Ortiz JV, Cioslowski J, Fox DJ (2009) Gaussian Inc, Wallingford
Guloy A, Ramlau R, Tang Z, Schnelle W, Baitinger M, Grin Y (2006) A quest-free germanium clathrate. Nature 443:320–323
Haag R, Schröder D, Zywietz T, Jiao H, Schwarz H, Von Schleyer PR, de Meijere AT (1996) The long elusive acepentalene – experimental and theoretical evidence for its existence. Angew Chem 35:1317–1319
Haag R, Schüngel F-M, Ohlhorst B, Lendvai T, Butenschön H, Clark T, Noltemeyer M, Haumann T, Boese R, de Meijere A (1998) Syntheses, structures, and reactions of highly strained dihydro- and tetrahydroacepentalene derivatives. Chem Eur J 4:1192–1200
Haddon RC (1987) Rehybridization and π-orbital overlap in nonplanar conjugated organic molecules: π-orbital axis vector (POAV) analysis and three-dimensional hückel molecular orbital (3D-HMO) theory. J Am Chem Soc 109:1676–1685
Haddon RC (1990) Measure of nonplanarity in conjugated organic molecules: which structurally characterized molecule displays the highest degree of pyramidalization? J Am Chem Soc 112:3385–3389
Han X, Zhou S-J, Tan Y-Z, Wu X, Gao F, Liao Z-J, Huang R-B, Feng Y-Q, Lu X, Xie S-Y, Zheng L-S (2008) Crystal structures of saturn-like $C_{50}Cl_{10}$ and pineapple-shaped $C_{64}Cl_4$: geometric implications of double- and triple-pentagon-fused chlorofullerenes. Angew Chem Int Ed 47:5340–5343
Krüger A, Kataoka F, Ozawa M, Fujino T, Suzuki Y, Aleksenskii AE, Vul' AYA, Ōsawa E (2005) Unusually tight aggregation in detonation nanodiamond: identification and disintegration. Carbon 43:1722–1730
Kuck D (2006) Functionalized aromatics aligned with the three Cartesian axes: extension of centropolyindane chemistry. Pure Appl Chem 78:749–775
Kyani A, Diudea MV (2012) Molecular dynamics simulation study on the diamond D_5 substructures. Central Eur J Chem 10(4):1028–1033
Meier WM, Olson DH (1992) Atlas of zeolite structure types, 3rd edn. Butterworth-Heinemann, London

Nagy CL, Diudea MV (2005) JSChem. Babes–Bolyai University, Cluj
Nagy CL, Diudea MV (2009) NANO-Studio software. Babes-Bolyai University, Cluj
Newkome GR, Yao Z, Baker GR, Gupta VK (1985) Micelles. Part 1. Cascade molecules: a new approach to micelles. A [27]-arborol. J Org Chem 50:2003–2004
Pan BF, Cui DX, Xu P, Huang T, Li Q, He R, Gao F (2007) Cellular uptake enhancement of polyamidoamine dendrimer modified single walled carbon nanotubes. J Biomed Pharm Eng 1:13–16
Paquette LA, Balogh DW (1982) An expedient synthesis of 1,16-dimethyldodecahedrane. J Am Chem Soc 104:774–783
Paquette LA, Vazeux M (1981) Threefold transannular epoxide cyclization. Synthesis of a heterocyclic C_{17}-hexaquinane. Tetrahedron Lett 22:291–294
Prinzbach H, Wahl F, Weiler A, Landenberger P, Wörth J, Scott LT, Gelmont M, Olevano D, Sommer F, Issendoef B (2006) C_{20} carbon clusters: fullerene-boat-sheet generation, mass selection, photoelectron characterization. Chem Eur J 12:6268–6280
Schwarz U, Wosylus A, Böhme B, Baitinger M, Hanfland M, Grin Y (2008) A 3D network of four-bonded germanium: a link between open and dense. Angew Chem Int Ed 47:6790–6793
Szefler B, Diudea MV (2012) On molecular dynamics of the diamond D_5 seed. Struct Chem 23(3):717–722
Tang MX, Redemann CT, Szoka FC Jr (1996) In vitro gene delivery by degraded polyamidoamine dendrimers. Bioconjug Chem 7:703–714
Tomalia DA (1993) Starburst™/cascade dendrimers: fundamental building blocks for a new nanoscopic chemistry set. Aldrichim Acta 26:91–101
Wahl F, Weiler A, Landenberger P, Sackers E, Voss T, Haas A, Lieb M, Hunkler D, Worth J, Knothe L, Prinzbach H (2006) Towards perfunctionalized dodecahedranes – en route to C_{20} fullerene. Chem Eur J 12:6255–6267
Zywietz TK, Jiao H, Schleyer PR, de Meijere A (1998) Aromaticity and antiaromaticity in oligocyclic annelated five-membered ring systems. J Org Chem 63:3417–3422